DAMPING OF MICRO ELECTROSTATIC TORSION MIRROR CAUSED BY AIR-FILM VISCOSITY

Norio Uchida, Kiyotaka Uchimaru, Minoru Yonezawa and Masayuki Sekimura
Mechanical Systems Laboratory, Corporate Research & Development Center, Toshiba Corporation
1, Komukai Toshiba-cho, Saiwai-ku, Kawasaki, 212-8582, Japan
Tel: +81-44-549-2374, FAX: +81-44-520-2057, e-mail: norio.uchida@toshiba.co.jp

ABSTRACT

A method of analyzing the damping characteristics of electrostatically driven torsion mirror actuators which have deep grooves on their electrodes is described. The damping force is caused by viscous friction of the gas film between a moving mirror plate and the electrodes. The grooves decrease the damping force and enable the moving plate to be driven at high speed and low driving voltage. To calculate the damping force correctly, it is necessary to consider the viscous friction not only on the moving plate and electrodes, but also on the sidewalls of the grooves. For that purpose, the idea of hydraulic mean depth is introduced and is applied to the Reynolds equation. The calculated damping force shows good agreement with the measured damping force of the developed torsion mirror actuator for optical heads.

INTRODUCTION

Electrostatic torsion mirror actuators and optical scanners fabricated by IC-based micromachining techniques are being developed in order to realize small size, low cost and high performance optical information equipment such as optical disk drives and bar code readers [1-6]. In these actuators, there are some cases where it is difficult to drive the moving plate at high speed and low voltage because of the strong damping force caused by the viscous friction (squeeze action) of the thin gas-film between the moving mirror plate and the electrodes. Therefore, it is important to not only decrease the squeeze action but to also understand the damping force correctly in these actuators.

To decrease the squeeze action, grooves are fabricated on the electrodes in our micro electrostatic torsion mirror actuator [5, 6]. The grooves decrease the area of the electrodes, resulting in the decrease of the driving force of the mirror plate. Therefore, it is necessary to fabricate large aspect ratio grooves with a relatively deep depth compared with the width. If the squeeze action of the gas-film for the actuator with deep and narrow grooves on the electrodes is calculated by conventional lubrication theory (Reynolds equation [7, 8]), the calculated results have unacceptable error, because the viscous friction on the sidewalls of grooves is ignored in Reynolds equation, which is derived under the assumption that the lubrication plane varies smoothly. In this article, a new method for approximation analysis of the squeeze action for the micro electrostatic torsion mirror actuator with grooves is described and the calculated damping force, which shows good agreement with the experimental results, is discussed.

ANALYSIS METHOD

The analysis model is shown in Fig. 1. Time-dependent pressure distribution in the gas-film is analyzed when the moving plate vibrates with the angle of $\theta=\theta_0\sin(2\pi ft)$. First, we consider the physical meaning of the Reynolds equation to introduce the viscous friction on the sidewalls of the grooves. The Reynolds equation is expressed by

$$\frac{\partial \rho h}{\partial t} = -\frac{1}{2}\frac{\partial}{\partial x}(\rho h V_x) + \frac{1}{12\mu}\frac{\partial}{\partial x}(\rho h^3 \frac{\partial p}{\partial x}) + \frac{1}{12\mu}\frac{\partial}{\partial y}(\rho h^3 \frac{\partial p}{\partial y}) \quad (1)$$

$$V_z = \frac{\partial h}{\partial t} + V_x \frac{\partial h_a}{\partial x} \quad (2)$$

where, p is pressure, ρ is density, μ is viscosity and t is time. h is the gap between the mirror plate and electrodes, including the groove depth, and h_a is the gap without groove depth. V_z and V_x are the velocity components of

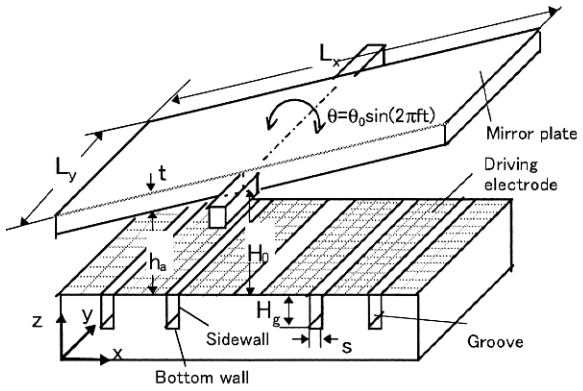

Figure 1: Electrostatic torsion mirror actuator

the mirror plate in the z and x directions, respectively. The Reynolds equation (1) multiplied by $\Delta x\Delta y$ can be rewritten as follows,

$$h\frac{\partial \rho}{\partial t}\Delta x\Delta y = -\rho\frac{\partial h}{\partial t}\Delta x\Delta y - \frac{1}{2}\left[(\rho h V_x)_{x+\frac{1}{2}\Delta x} - (\rho h V_x)_{x-\frac{1}{2}\Delta x}\right]\Delta y + \left[\left\{\frac{h^3}{12\mu}\rho\frac{\partial p}{\partial x}\right\}_{x+\frac{1}{2}\Delta x} - \left\{\frac{h^3}{12\mu}\rho\frac{\partial p}{\partial x}\right\}_{x-\frac{1}{2}\Delta x}\right]\Delta y + \left[\left\{\frac{h^3}{12\mu}\rho\frac{\partial p}{\partial y}\right\}_{y+\frac{1}{2}\Delta y} - \left\{\frac{h^3}{12\mu}\rho\frac{\partial p}{\partial y}\right\}_{y-\frac{1}{2}\Delta y}\right]\Delta x. \quad (3)$$

Subdividing the gas-film into small volumes as shown in Fig. 2, we consider the physical meaning of Eq.(3) in the control volume shown by dotted lines. The left-hand side expresses the mass increase per unit time due to the density change in the control volume. The first term of the right-hand side represents the mass flow of the gas which flows out of the boundary ABCD in the z direction during a unit of time due to the movement of the mirror plate. The second term is the mass difference of the gas which flows in and out of the control volume in the x direction through the boundaries ABFE and CDLK due to the velocity component V_x. The third and forth terms show the mass difference of the gas which flows in and out of the control volume through the boundaries ABFE and CDLK, and ADLIHE and BCKJGF during a unit time due to the pressure gradient.

Meanwhile, the term of $-(h^3/12\mu)\rho(\partial p/\partial y)\Delta x$ represents the mass flow of the gas which flows between upper and bottom plates in the y direction with the gap of h and width of Δx due to the pressure gradient of $-\partial p/\partial y$. Though the term of $-(h^3/12\mu)\rho(\partial p/\partial y)\Delta x$ contains the viscous friction on the upper and bottom plates, it does not contain the viscous friction on the sidewalls of the grooves, because the Eqs. (1) and (3) are derived from the Navier-Stokes equation under the assumption that the lubrication plane varies smoothly. Therefore, if calculation is conducted substituting $h=h_a+H_g$ for the gap at the grooves, the result would have unacceptable error. As the grooves become deeper, the viscous friction on the sidewalls of the grooves becomes larger than that on the upper and bottom plates, and so the error of the calculated results becomes larger.

In order to strictly calculate the viscous friction on the sidewalls of the grooves, three-dimensional analysis which requires massive calculations would be necessary. Therefore, in this article, the viscous friction on the sidewalls of grooves is introduced to the Reynolds equation by applying the idea of hydraulic mean depth [9] (effective groove depth) for the flow in the grooves.

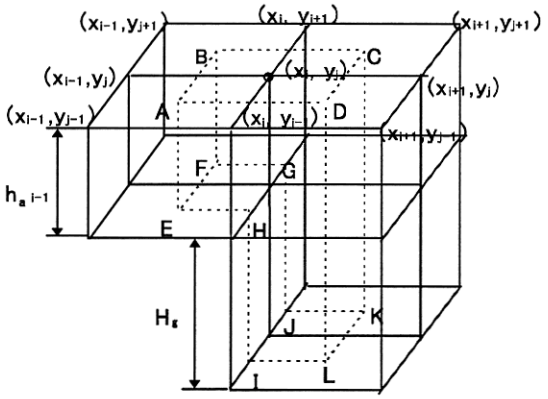

Figure 2: Control volume between the mirror plate and electrodes

The mass flow q_1 between two plates with the gap of h and the width of s due to the pressure gradient of $-dp/dy$ can be expressed as follows.

$$q_1 = -\frac{h^3}{12\mu}\rho\frac{dp}{dy}s \quad (4)$$

On the other hand, the mass flow q_2 for an open channel or a pipe with a rectangular cross section can be represented by

$$q_2 = -k\frac{m^2}{2\mu}A\rho\frac{dp}{dy}, \quad and \quad m = \frac{A}{U} \quad (5)$$

where, A is the area of the cross section and U expresses the wetted perimeter (the length along which fluid touches the wall in the cross section), and k is a constant. Expressing the average gap between the mirror plate and the electrodes by H_0, and the depth and the width of the grooves by H_g and s, respectively, A and U are written as $A=s(H_0+H_g)$ and $U=2(H_g+s)$, and then,

$$m = \frac{s(H_g+H_0)}{2(H_g+s)} \quad (6)$$

Substituting Eq.(6) into Eq.(5), and expressing with the same form as Eq. (4),

$$q_2 = -k\frac{s^2(H_g+H_0)^3}{8\mu(H_g+s)^2}\rho\frac{dp}{dy}s. \quad (7)$$

Putting $q_1=q_2$, and using the relation of $h= H_0$ when $H_g=0$, $k=2/3$ is obtained. Therefore, h can be represented by the following relation.

$$h = \sqrt[3]{\frac{s^2}{(H_g+s)^2}}(H_g+H_0) \quad (8)$$

Equation (8) expresses the effective gap which makes the mass flow q_1 between the upper and bottom plates in the grooves equal to the mass flow q_2 in which the viscous friction on the sidewalls of the grooves is considered. Therefore, the effective groove depth H_{geff}

can be written as follows.

$$H_{g_{eff}} = h - H_0 \tag{9}$$

Thus, when h_a+H_{geff} is used instead of h_a+H_g for the flow along the grooves (fourth term of right-hand side in Eq.(3)), the pressure distribution of the gas-film including the effect of the viscous friction on the sidewalls of the grooves can be calculated.

NUMERICAL CALCULATION METHOD

As the isothermal change ($\rho \propto p$) can be assumed in the gas-film, ρ is replaced with p in Eq.(3). Subdividing the gas-film into equal $N\times M$ subareas (i=0–N, j=0–M), the lengths of each subarea are defined as $\Delta x=x_{i+1}-x_i$ and $\Delta y=y_{i+1}-y_i$ in the x and y directions, respectively, as shown in Fig. 2. The time axis is expressed by $t=n\Delta t$. The functions $p(t,x,y)$, $h_a(t,x)$, $V_x(t,x)$ *and* $V_z(t,x)$ defined at the nodes ($n\Delta t$, $i\Delta x$, $j\Delta y$) are designated by $p_{i,j}^{\ n}$, $ha_i^{\ n}$, $V_{xi}^{\ n}$ *and* $V_{zi}^{\ n}$, where $h_{ai}^{\ n}$, $V_{xi}^{\ n}$ and $V_{zi}^{\ n}$ are given values.

Nonlinear equation (3) is converted into linear difference equations by Lees approximation method [10]. Defining $p=p_a+\Delta p$ (p_a: periphery pressure), the pressure variation Δp is small enough, that is, $\Delta p/p_a$ <<1. Therefore, the known values $p_{i,j}^{\ n}$ which are calculated one step earlier are substituted for p in the terms $p(\partial p/\partial x)$ and $p(\partial p/\partial y)$ of Eq.(3). Furthermore, the differential terms $\partial p/\partial t$, $\partial p/\partial x|_{x+\Delta x/2}$, $\partial p/\partial y|_{y+\Delta y/2}$,... can be expressed by $(p_{i,j}^{\ n+1}-p_{i,j}^{\ n})/\Delta t$, $(p_{i+1,j}^{\ n+1}-p_{i,j}^{\ n+1})/\Delta x$, $(p_{i,j+1}^{\ n+1}-p_{i,j}^{\ n+1})/\Delta y$,..., respectively. Therefore, when the following relations in the control volume shown by the dotted lines in Fig. 2 are substituted into Eq.(3),

$$h\frac{\partial p}{\partial t}\Delta x\Delta y = (h_{ai}^{\ n}+\frac{1}{2}H_g)\frac{p_{i,j}^{n+1}-p_{i,j}^{n}}{\Delta t}\Delta x\Delta y\,,$$

$$p\frac{\partial h}{\partial t}\Delta x\Delta y = p_{i,j}^{n}(V_{zi}^{\ n}-V_{xi}^{n}\frac{dh_{ai}^{\ n}}{dx})\Delta x\Delta y\,,$$

$$\vdots$$

$$\frac{h^3}{12\mu}p\frac{\partial p}{\partial x}\bigg|_{x+\frac{1}{2}\Delta x}\Delta y = \frac{1}{12\mu}\left\{\frac{1}{2}(h_{ai+1}^{\ n}+h_{ai}^{\ n})+H_g\right\}^3 \times\frac{(p_{i+1,j}^{n}+p_{i,j}^{n})}{2}\frac{(p_{i+1,j}^{n+1}-p_{i,j}^{n+1})}{\Delta x}\Delta y\,,$$

$$\vdots$$

$$\frac{h^3}{12\mu}p\frac{\partial p}{\partial y}\bigg|_{y-\frac{1}{2}\Delta y}\Delta x = \frac{1}{12\mu}\left\{\frac{1}{2}(h_{ai}^{\ n})^3+\frac{1}{2}(h_{ai}^{\ n}+H_{g_{eff}})^3\right\} \times\frac{(p_{i,j}^{n}+p_{i,j-1}^{n})}{2}\frac{(p_{i,j}^{n+1}-p_{i,j-1}^{n+1})}{\Delta y}\Delta x \tag{10}$$

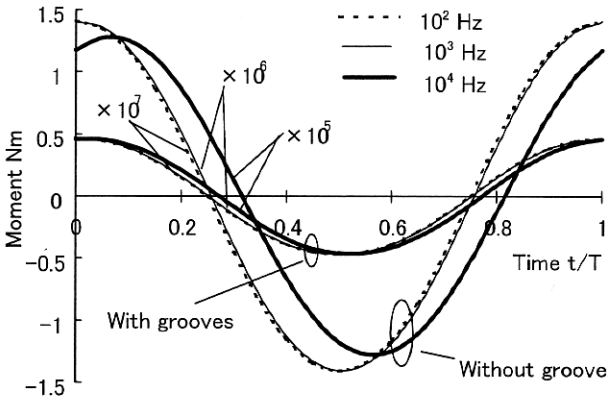

Figure 3: Moment caused by squeeze action at various frequencies (T : period)

Eq.(3) can be rewritten as follows,

$$a_{i,j}p_{i+1,j}^{n+1}+b_{i,j}p_{i,j}^{n+1}+c_{i,j}p_{i-1,j}^{n+1}+d_{i,j}p_{i,j+1}^{n+1}+e_{i,j}p_{i,j-1}^{n+1}=f_{i,j} \tag{11}$$

where, $a_{i,j}$, $b_{i,j}$,..., and $f_{i,j}$ are expressed by Δt, Δx, Δy, $h_{ai}^{\ n}$, $V_{xi}^{\ n}$, $V_{zi}^{\ n}$ and $p_{i,j}^{\ n}$. Solving these $(N-1)\times(M-1)$ linear equations with the following $2(N+1)+2(M-1)$ boundary conditions,

$$p_{i,0}^{n+1}=p_{i,M}^{n+1}=p_a\,,\quad p_{0,j}^{n+1}=p_{N,j}^{n+1}=p_a\,,\quad (i=0-N, j=1-(M-1)) \tag{12}$$

$p_{i,j}^{\ n+1}$ at $t=(n+1)\Delta t$ are obtained.

CALCULATED RESULTS

Effect of frequency

The time-dependent moment which arises from the pressure variation $\Delta p_{i,j}(t,x.y)$ due to the squeeze action is shown in Fig. 3 when the mirror plate is vibrated with the function of $\theta=(2H_1/L_x)\sin(2\pi ft)$, where L_x=3 mm, L_y=2.5 mm, H_0=7 μm, and μ=1.82×10^{-5} Ns/m^2. H_1 (=1 μm) is the amplitude of the tip of the mirror plate. A parameter is the frequency of vibration (10^2, 10^3, 10^4 Hz). The moment in the case that two grooves of $H_g=s$= 100 μm are fabricated at the positions of $L_x/4$ and $3L_x/4$ is also shown. The values of the vertical axis are multiplied by 10^7 at $f=10^2$ Hz, by 10^6 at $f=10^3$ Hz, and by 10^5 at $f=10^4$ Hz, and so the value of the moment at t=0 and $f=10^2$ Hz is 1.41×10^{-7} Nm. From this figure, the moment can be expressed by $M\propto f\cos(2\pi ft)$ except for $f=10^4$ Hz without grooves. Although a phase lag due to the effect of the compressibility of the gas occurs in the moment without grooves at $f=10^4$ Hz, the phase lag disappears if grooves are fabricated. Therefore, the moment is directly proportional to the velocity of the mirror plate, and the amplitude of the moment is in proportion to the frequency. Thus, after this,

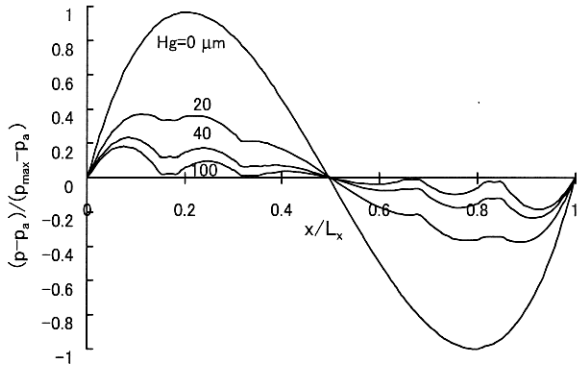

Figure 4: Pressure distribution in the x direction (s=100 μm, t/T=1.0 and $y=L_y/2$)

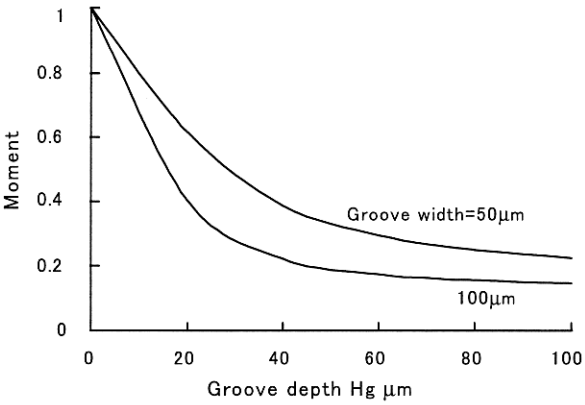

Figure 5: Relation between the moment and the groove depth (the number of grooves=4)

calculations are carried out only at $f=10^3$ Hz, and the moment at other frequencies is obtained by a conversion using the relation that moment is proportional to the frequency of vibration.

Effect of groove depth

The pressure distributions $\Delta p(x,L_y/2)$ at t/T=1 (T: period) are shown in Fig. 4 when 100 μm-wide grooves are fabricated in the positions of $L_x/6$, $L_x/3$, $2L_x/3$ and $5L_x/6$. The vertical axis is non-dimensional values divided by the peak pressure without grooves. The pressure takes a maximum or minimum value at the position of about $L_x/5$ from both ends in the case of no groove. If grooves are fabricated, the deeper the depth of the grooves, the smaller the pressure variation. Moreover, the pressure distribution in the grooves becomes almost uniform. This fact shows that the assumption which is used to derive H_{geff} is reasonable.

Figure 5 shows the moment calculated from the pressure distribution in Fig. 4. The vertical axis shows non-dimensional values divided by the moment without grooves. Comparing the moment with grooves of the 50

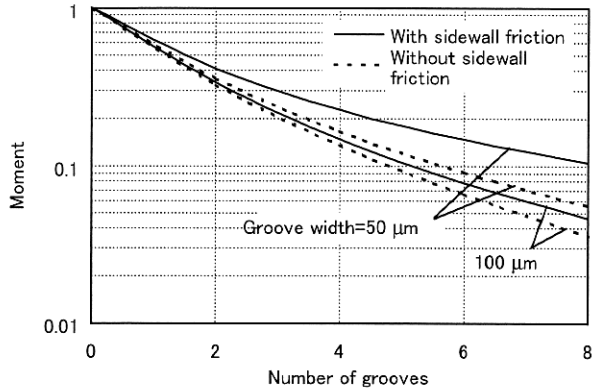

Figure 6: Relation between the moment and the number of grooves (H_g=100 μm)

μm-width and 100 μm-depth and that with grooves of the 100 μm-width and 50 μm-depth, the moment is smaller for the wider grooves, for grooves of equal sectional area.

Effect of the number of grooves

Figure 6 shows the moment with 100 μm-deep grooves, when the number of grooves (N) is varied from 2 to 8. The moment, not considering the effect of the viscous friction on the sidewalls of the grooves, is also plotted by dotted lines. As a matter of course, the moment due to the squeeze action decreases with the increase of N. The difference between the solid line and dotted line is larger in the 50 μm-width grooves (aspect ratio=2) than in the 100 μm-width grooves (aspect ratio=1). This means that the effect of the viscous friction on the sidewalls is much more significant in the grooves with a large aspect ratio.

The case that total groove width is constant

Although the moment due to the squeeze action decreases if the number of grooves increases while a

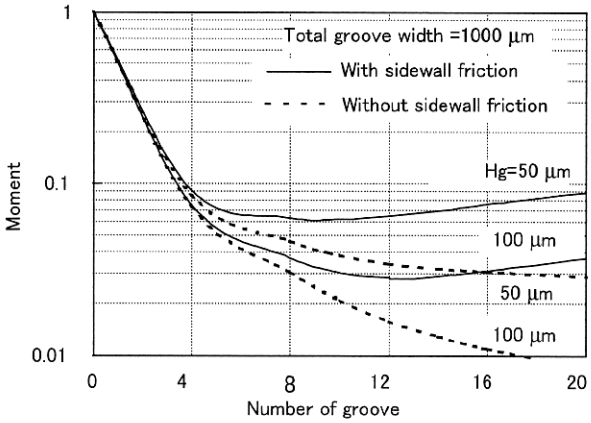

Figure 7: Moment when the total groove width (TGW) is 1000 μm (TGW=$s\times N$)

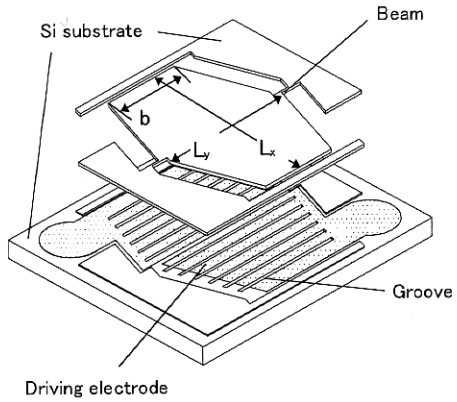

Figure 8: Schematic view of the developed mirror actuator

Table 1: Dimensions of the developed mirror actuator

Mirror plate	L_x	3.03 mm	Electrode plate	s	80, 120 μm
	L_y	2.45 mm		N	12
	b	1.38 mm		s×N	960 μm 1440 μm
	t	60 μm		H_g	100 μm
	I	5.33×10^{-13} kgm^2	Gap	H_0	7 μm

t: Thickness, N: Number of grooves

Table 2: Damping coefficients for various total groove widths at the frequency of 1000Hz

s×N μm	c Nms
0	2.01×10^{-7}
600	9.86×10^{-9}
1000	4.61×10^{-9}
1440	2.41×10^{-9}

constant groove width is maintained, the driving torque of the mirror plate also decreases. Therefore, the variation of the moment is shown in Fig. 7, when N is varied from 2 to 20 under the condition of a constant total groove width, i.e., (*groove width*) × (*number of grooves*)=1000 μm. The moment without considering the viscous friction on the sidewalls of the grooves is also shown by dotted lines. When the viscous friction on the sidewalls is not considered, the moment decreases monotonously with increasing N and becomes 1/116 of the moment without grooves when N=20 and H_g=100 μm. The reason is that the viscous friction in the grooves becomes small even if the groove width is narrow because the friction on the sidewalls of the grooves is ignored. On the other hand, considering the friction on the sidewalls of the grooves, the moment takes a minimum value at the number of grooves between 10 and 12. The reason is that as the number of grooves increases, the effective groove depth H_{geff} is smaller so that the pressure in the grooves does not decrease much. Thus, the minimum value of the moment does not decrease lower than 1/34 of the moment without grooves. The moment in the case that

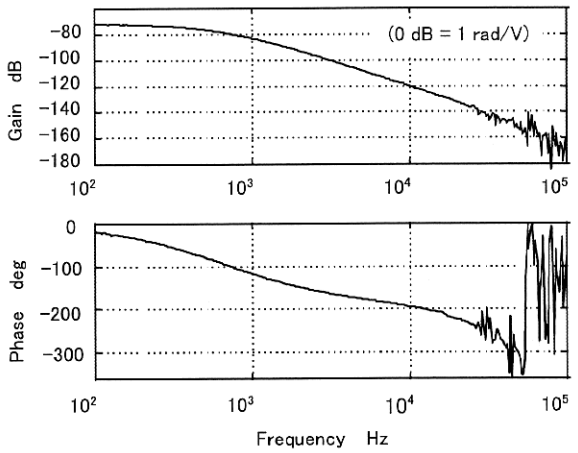

Figure 9: Frequency response of the developed mirror actuator (N=12, s=80 μm)

the viscous friction on the sidewalls is considered becomes about twice as larger as the moment without the viscous friction on the sidewalls of grooves, when N=12 and H_g=100 μm. The moment for H_g=50 μm takes a minimum value at a smaller number of grooves than that for H_g=100 μm.

DAMPING RATIOS

As mentioned above, the moment due to the squeeze action can be expressed by $M=M_0\cos(2\pi ft)$, when the angular displacement of the mirror plate is $\theta=\theta_0\sin(2\pi ft)$. Therefore, a damping coefficient c is represented by,

$$c=\frac{M}{\dot{\theta}}=\frac{M_0}{2\pi f\theta_0}. \tag{13}$$

M_0 is proportional to the frequency of vibration, and so the damping coefficient c is a constant value with no relation to the frequency. Expressing the moment of inertia of the mirror plate by I, the critical damping coefficient by c_c and natural frequency by f_0, the damping ratio ζ can be calculated by the following equation if f_0 is obtained by experiment.

$$\zeta=\frac{c}{c_c}=\frac{c}{4\pi f_0 I} \tag{14}$$

The shape and dimensions of the developed electrostatic torsion mirror actuator are shown in Fig. 8 and Table 1. The gap between the mirror plate and the electrodes is 7 μm. To decrease the damping force due to the viscosity of gas-film, twelve 100 μm-deep grooves are fabricated on the electrodes, corresponding to the above-mentioned analysis. A parameter is the total groove width of 960 μm and 1440 μm. The damping coefficient c of the actuator in the configuration of Fig. 8 is calculated under the condition of H_1=1 μm and f=10^3 Hz and is shown in Table 2.

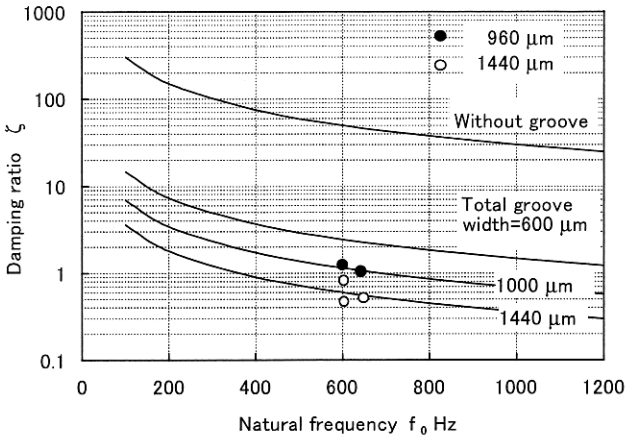

Figure 10: Experimental and calculated damping ratios of the developed mirror actuator

Figure 9 shows an example of experimental results of the transfer function from the driving voltage to the response angle for the actuator with a total groove width of 960 μm. The natural frequency and damping ratio are obtained as 630 Hz and 1.0, respectively, when the experimental result is identified using a quadratic transfer function.

Calculated and experimental damping ratios versus the natural frequency are shown in Fig. 10. The damping ratio was able to be measured only for the actuators with the total groove width of 960 μm and 1440 μm. With regard to the actuator without grooves, it was impossible to vibrate the mirror plate up to the natural frequency because of excessively strong damping force. In the calculated results, at f_0=600 Hz, the damping ratio without grooves is very large and ζ=50. It decreases to ζ=2.45 when the total groove width is 600 μm, and to ζ=1.15 and ζ=0.60 when the total groove widths are 1000 μm and 1440 μm, respectively. The calculated results show good agreement with experimental results though there is some dispersion in the experimental results.

CONCLUSION

A method of analyzing the damping force caused by the squeeze action of the gas film between the mirror plate and the electrodes of an electrostatic torsion mirror actuator has been developed. In particular, a method of analyzing the squeeze action in the case that deep grooves are fabricated on the electrodes in order to decrease the excessively strong damping force has been newly developed. The main conclusions are as follows:

(1)The damping force due to the squeeze action of the gas film decreases when grooves are fabricated on the electrodes. If calculations of the damping force are conducted using the conventional lubrication theory in which the viscous friction on the sidewalls of grooves is ignored, the calculated damping force has unacceptable error.

(2)In the case that (*groove width*)×(*number of grooves*) = *constant*, there is a number of grooves where the damping force takes a minimum value. In the developed mirror actuator, the number of grooves is between 10 and 12.

(3)The damping force calculated by the newly developed analysis method shows good agreement with the experimental results of the developed mirror actuators.

REFERENCES

[1] H. Fujita and K. J. Gabrier, "New Opportunities for Micro Actuators", Dig. Technical Papers, Transducers '91, (1991) pp. 14-20.

[2] T. Usuda and A. Umeda, "An Electrostaticlly Driven Torsional Resonator with Two Degrees of Freedom (1st Report)", J. JSPE, 62, 9 (1996) pp. 1292-1296 (in Japanese).

[3] Y. Ohtsuka, S. Akita, T. Hattori, T. Kounuma, and H. Nishikawa, "2-Dimensional Optical Scanner Applying Torsional Resonator With 3 Degrees of Freedom", T. IEE Japan, 116-E, 8 (1997) pp. 345-351 (in Japanese).

[4] S. W. Chung, J. W. Shin, Y. K. Kim, and B. S. Han, "Design and Fabrication of Micro Mirror Supported by Electroplated Nickel Posts", Transducers '95· Eurosensors IX (1995) pp. 312-315.

[5] M. Sekimura, M. Yonezawa, K. Uchimaru, A. Kasahara, and N. Uchida, "Electrostatic Torsion Mirror", Technical Digest of 16th Sensor and Symposium, (1998) pp. 167-170.

[6] M. Yonezawa, M. Sekimura, K. Uchimaru, N. Uchida, and A. Kasahara, "Electrostatic Torsion Mirror for Optical Disk Drives", Proc. MORIS-1999, pp.241-244.

[7] E. Kim, Y. Cho, and M. Kim, "Effect of Holes and Edges on the Squeeze Film Damping of Perforated Micromechanical Structure", Proc. MEMS-1999, pp. 296-301.

[8] K. Minami, T. Matsunaga and M. Esashi, "Simple Modeling and Simulation of the Squeeze Film Effect and Transient Response of the MEMS Device", Proc. MEMS-1999, pp. 338-343.

[9] H. Schlichting, "Boundary-Layer Theory", McGRAW-HILL, INC. (1979) p. 612 .

[10] W.A. Michael, "Approximate Methods for Time-Dependent Gas-Film Lubrication Problems", Trans. ASME, J. Appl. Mech., 30 (1963) pp.509-517.